Supplementary Information

Atomic-Scale Mechanisms of Interphase Formation at Lithium–Glassy Sulfide Electrolyte Interfaces

Rui Zhou[a], Luo Kun[a], and Qi An[a*]

[a] Department of Materials Science and Engineering, Iowa State University, Ames, Iowa 50011, United States

[*]Corresponding Author's Email: qan@iastate.edu

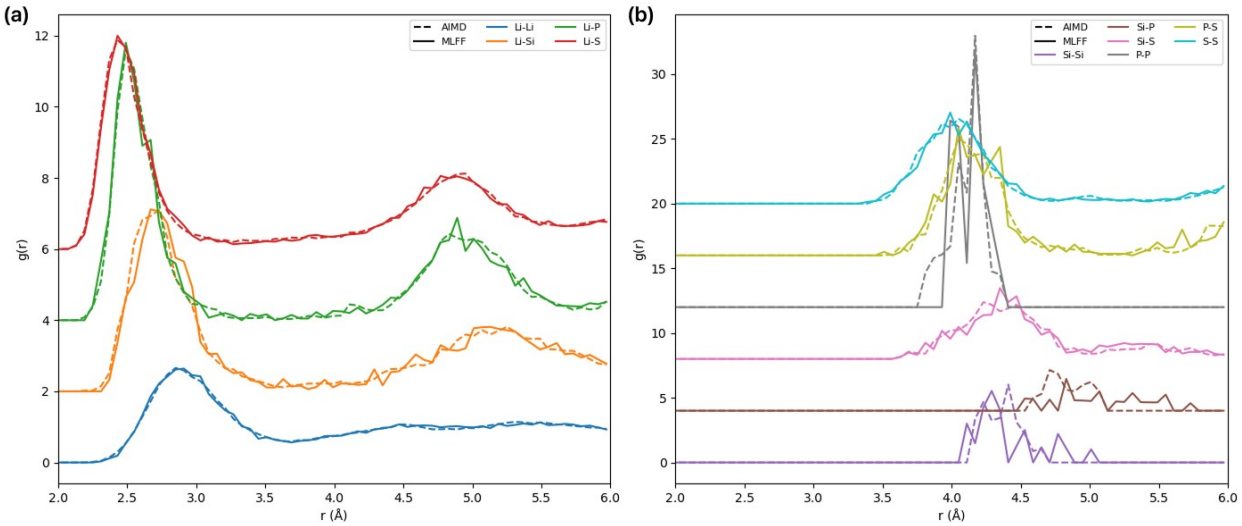

Figure S1. Comparison of the radial distribution functions of the $Li_{72}|Li_{12}Si_3P_2S_{17}$ validation system obtained from *ab initio* molecular dynamics (AIMD, dashed lines) and the machine learning force field (ML-FF, solid lines), showing good agreement between the two methods.

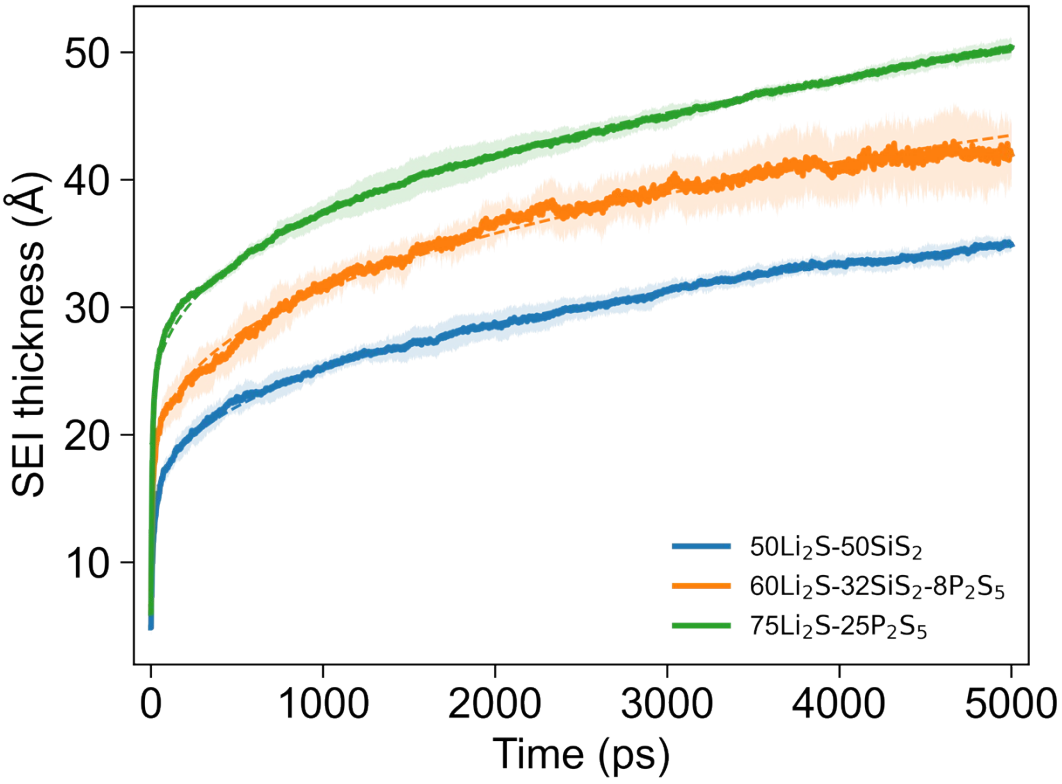

Figure S2. SEI thickness of all 3 composition during 5 ns simulation fitted with cubic root model.

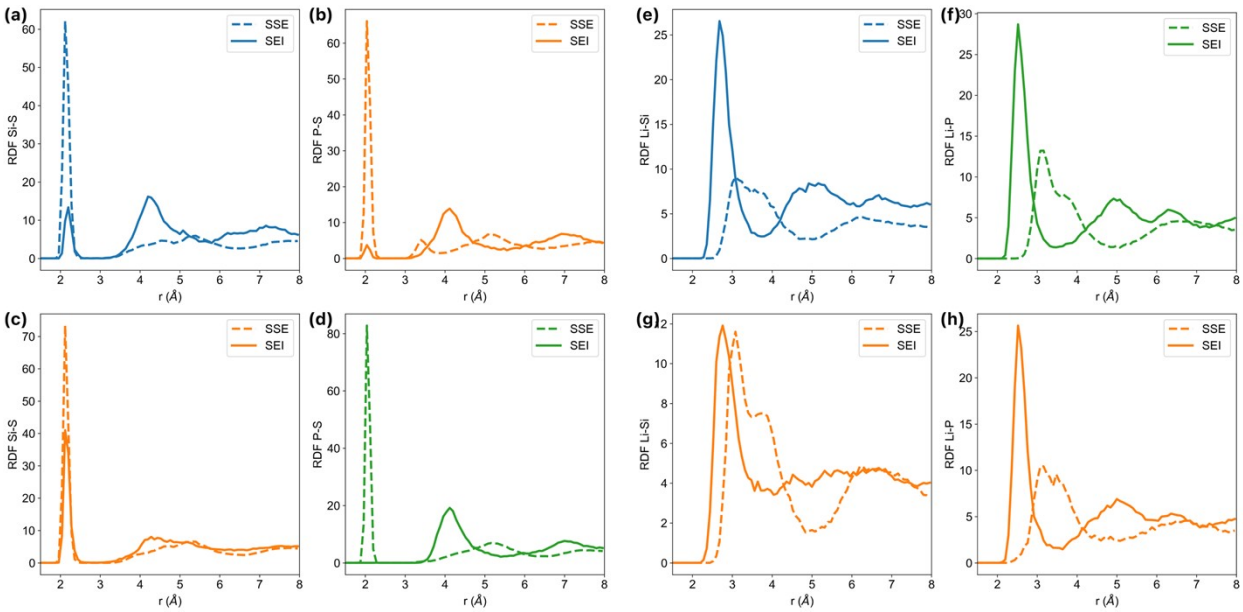

Figure S3. Radial distribution function (RDF) of Si-S, P-S, Li-Si, and Li-P pairs in bulk SSE and SEI regions for $50Li_2S$-$50SiS_2$ (LiSiS), $60Li_2S$-$32SiS_2$-$8P_2S_5$ (LiSiPS), and $75Li_2S$-$25P_2S_5$ (LiPS) systems: (a) Si-S pair in LiSiS, (b) P-S pair in LiSiPS, (c) Si-S pair in LiSiPS, (d) P-S pair in LiPS, (e) Li-Si pair in LiSiS, (f) Li-P pair in LiPS, (g) Li-Si pair in LiSiPS, (h) Li-P pair in LiSiPS.

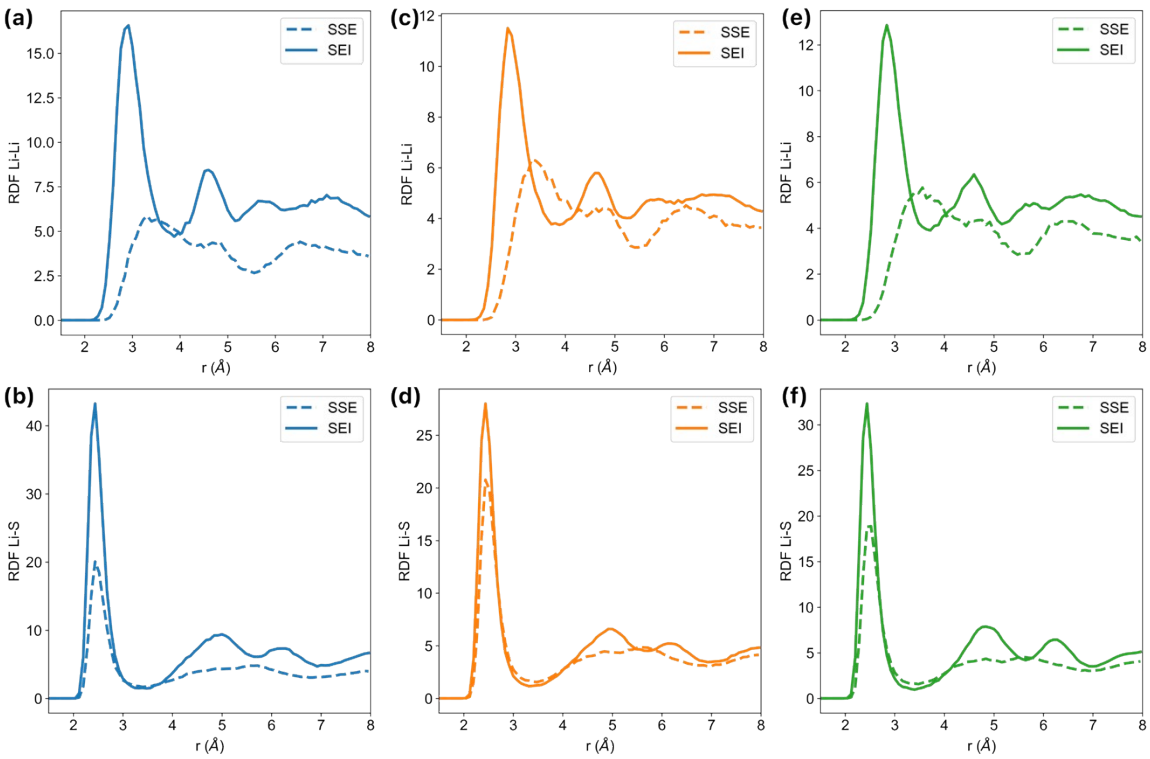

Figure S4. Radial distribution function of Li-Li and Li-Si pairs in bulk SSE and SEI regions for $50Li_2S$-$50SiS_2$ (LiSiS), $60Li_2S$-$32SiS_2$-$8P_2S_5$ (LiSiPS), and $75Li_2S$-$25P_2S_5$ (LiPS) systems: (a,b) LiSiS, (c,d) LiSiPS, and (e,f) LiPS.

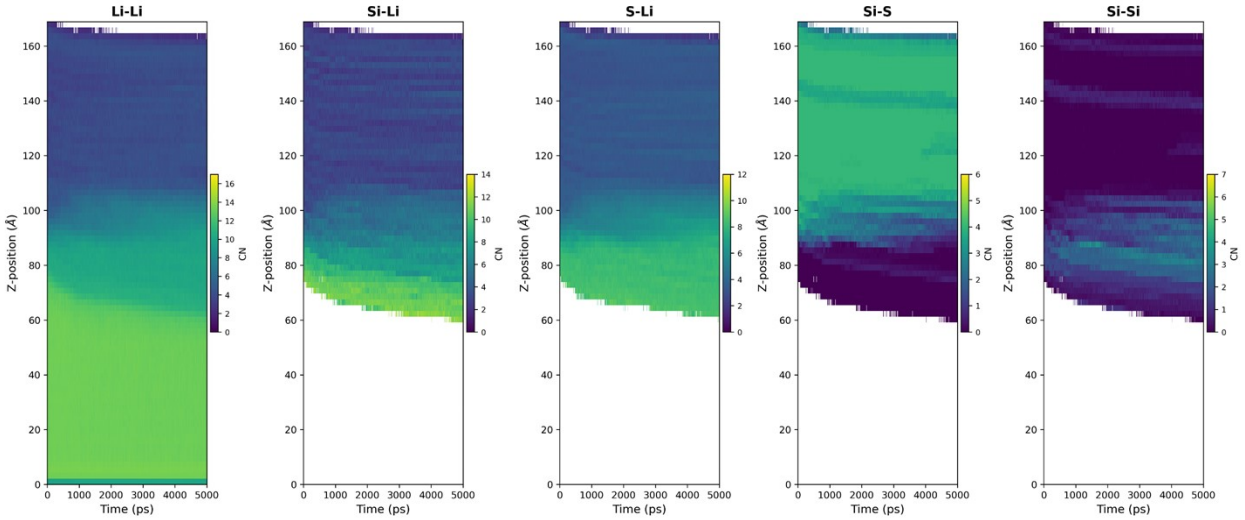

Figure S5. Time-dependent coordination number profiles of representative atomic pairs along the z-axis for the LiSiS compound.

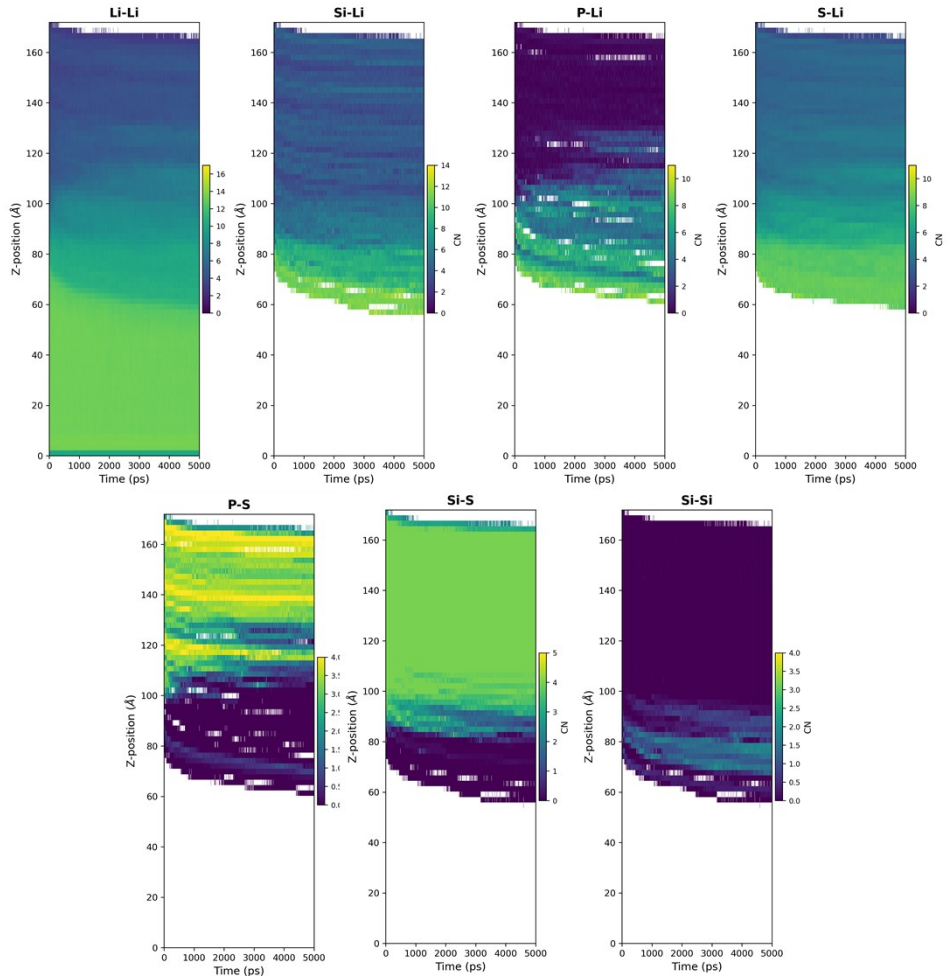

Figure S6. Time-dependent coordination number profiles of representative atomic pairs along the z-axis for the LiSiPS compound.

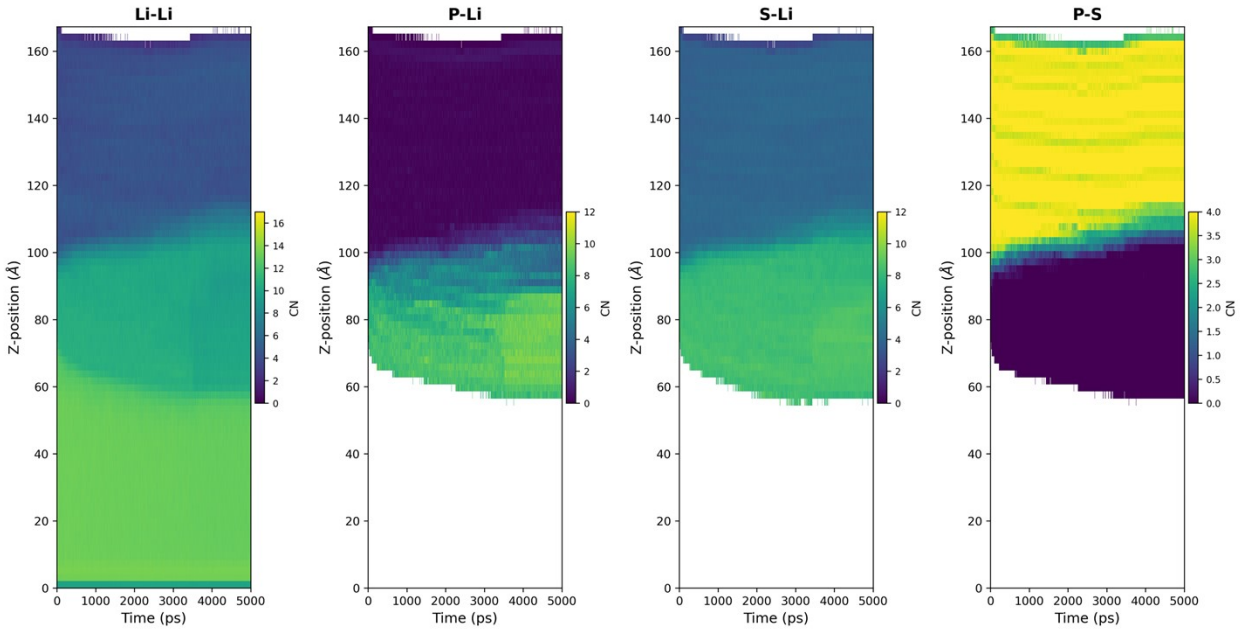

Figure S7. Time-dependent coordination number profiles of representative atomic pairs along the z-axis for the LiPS compound.

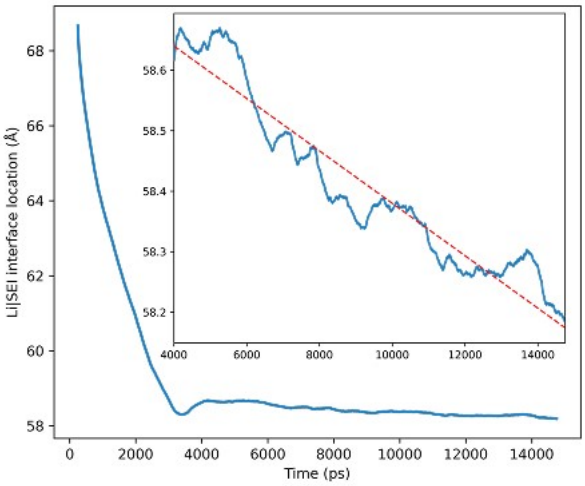

Figure S8. Li|SEI interface position of the formed crystallized SEI of Li|LiPS from the MD simulations.

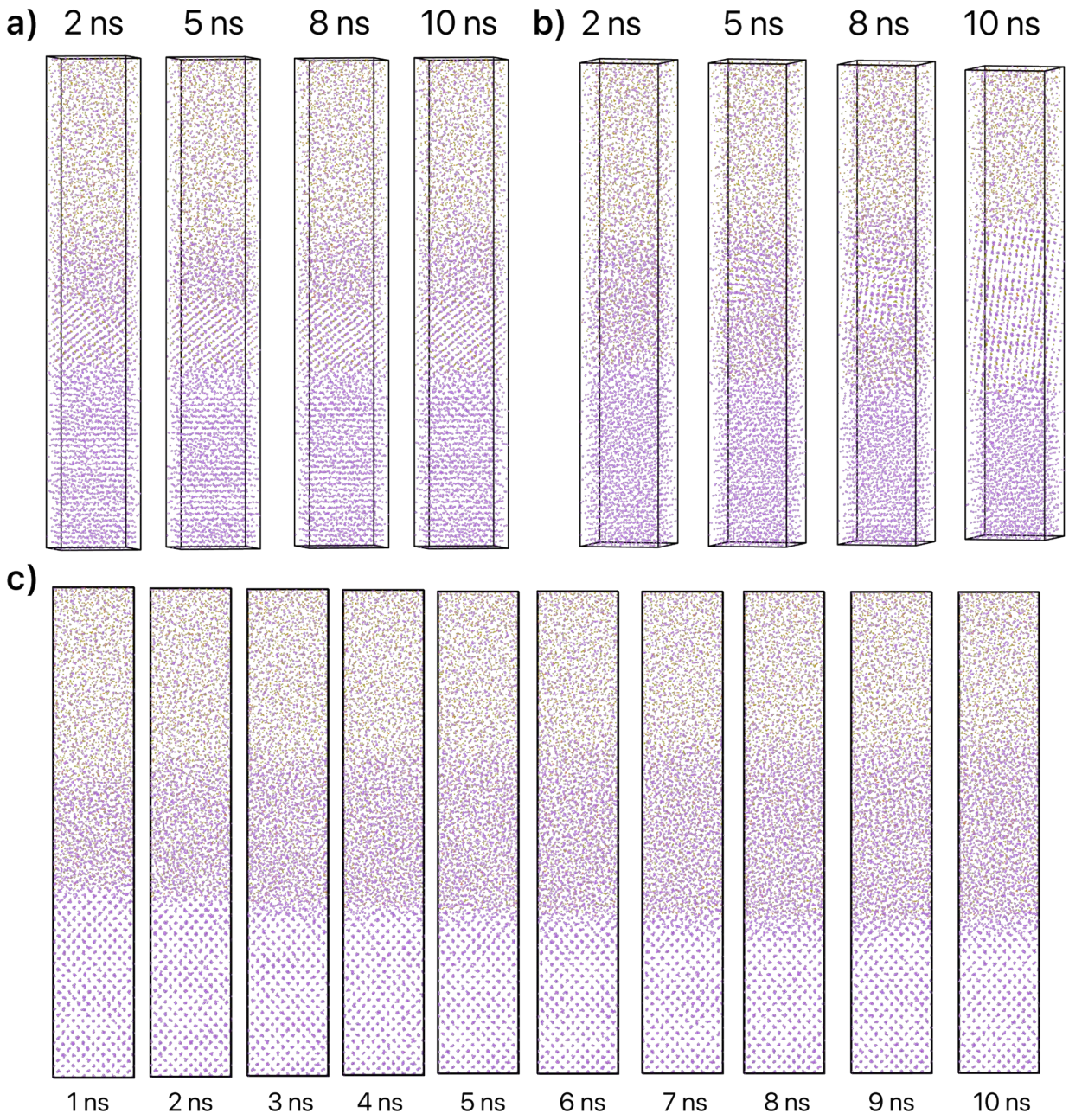

Figure S9. Snapshots of the Li|LPS interface evolution over 10 ns from reproducibility tests. The initial Li|LPS structure was chosen to be the same as the one that showed crystallization in the main manuscript, but different initial velocities were assigned. Panels (a) and (b) show two trajectories in which crystallization occurs, whereas panel (c) shows one trajectory as example in which the SEI remains amorphous.

Table S1. Coefficients of determination (R^2) for fitting SEI thickness evolution using different time-dependence models for the three compositions: $50Li_2S$-$50SiS_2$ (LiSiS), $60Li_2S$-$32SiS_2$-$8P_2S_5$ (LiSiPS), and $75Li_2S$-$25P_2S_5$ (LiPS).

	LiSiS	LiSiPS	LiPS
$t^{1/2}$	0.9926	0.9725	0.9973
$t^{1/3}$	0.9980	0.9887	0.9982
t^{n}	0.9980	0.9925	0.9927
$\ln t$	0.9659	0.9766	0.9553

Table S2. Root-mean-square errors (RMSEs) of different time-dependence models fitted on the first 25% of the SEI thickness evolution and evaluated on the remaining 75% for the three electrolyte compositions.

	LiSiS	LiSiPS	LiPS
$t^{1/2}$	2.1680	3.6890	1.8773
$t^{1/3}$	0.3433	1.1260	0.5538
t^{n}	0.7990	4.9172	0.9821